

## Structural, Infra-red and Morphological Effect of Sm<sup>3+</sup> Doped Barium Titanate Nanoparticles

<sup>\*1,2</sup>Lariski, F. M., <sup>2</sup>Zangina, T., <sup>2</sup>Ndikilar, C. E., <sup>2</sup>Mohammed, J.

<sup>1</sup>Department of Physics, Faculty of Science, Yobe State University, Damaturu, Yobe State, Nigeria

<sup>2</sup>Department of Physics, Faculty of Science, Federal University, Dutse, Jigawa State, Nigeria

\*Corresponding author's email: [fmusalariski@gmail.com](mailto:fmusalariski@gmail.com)

### ABSTRACT

Barium titanate (BaTiO<sub>3</sub>) ceramics, prepared by the sol-gel method, were investigated considering the influence of the doped samarium concentration. Undoped BaTiO<sub>3</sub> and doped BaTi<sub>1-x</sub>Sm<sub>x</sub>O<sub>3</sub> (x = 0.0, 0.1, 0.2) were characterized by using X-ray diffraction (XRD), Fourier Transform Infrared Spectroscopy (FTIR), Field Emission Scanning Electron Microscopy (FESEM), and Energy Dispersive X-ray Spectroscopy (EDX). XRD results shows the replacement of Ti<sup>4+</sup> ions (0.605 Å) by the bigger Sm<sup>3+</sup> ions (0.958 Å) leading to the variation in cell parameter demonstrating the increase in lattice parameter with the increase of Sm content. The calculated tolerance value was 0.952 considering Sm-at B-site for BaTi<sub>1-x</sub>Sm<sub>x</sub>O<sub>3</sub> indicating a cubic perovskite structure, a strong absorption peak for pure BT powder is observed around 493 cm<sup>-1</sup>, signifying the stretching of normal vibration for Ti-O octahedron. Another absorption peaks for the same mode are observed at 503 and 512 cm<sup>-1</sup> for x = 0.1 and 0.2 respectively. FESEM show that the particles follow a normal distribution, with average particle sizes of 73.5 nm and 70.5 nm for x = 0.0 and x = 0.2 respectively, that is to say that the particle size decreases slightly with Sm concentrations, EDX spectra confirms the presence of Ba, Ti, O and dopant in our prepared sample of the same constituents.

### Keywords:

Barium titanate,  
Infra-red,  
Morphological,  
Nanoceramics,  
Structural.

### INTRODUCTION

The exceptional ferroelectric, pyroelectric, piezoelectric, dielectric, elastic, and electro-optic properties of alkaline earth titanates, particularly BaTiO<sub>3</sub> and SrTiO<sub>3</sub>, have made research on these nanostructures very important. Therefore, these materials are crucial for technical devices including nonvolatile random-access memory (NVRAM) and photonic crystals as well as transducers, capacitors, actuators, thermistors, and other devices (Dutta et al., 2014).

Ferroelectric BaTiO<sub>3</sub> is a substance with a positive temperature coefficient, a high dielectric constant, and little dissipation. Pure BaTiO<sub>3</sub> ceramics do not, however, have dielectric characteristics that are suitable for commercial use. Effectively modifying the dielectric characteristics is possible with cationic replacements at the Ba<sup>2+</sup> and Ti<sup>4+</sup> sites (Li et al., 2017).

BaTiO<sub>3</sub> is a ferroelectric oxide that, when heated over 130 °C, transforms from a ferroelectric tetragonal phase to a paraelectric cubic phase (Smith et al., 2008).

One of the most crucial ceramic materials in electronics is tetragonal BaTiO<sub>3</sub>, which is a ferroelectric perovskite

at ambient temperature (Paunovic et al., 2016). Due to its high dielectric constant and wide range of applications, such as capacitors, sensors, actuators, power transmission devices, memory devices, and high energy storage devices, the BaTiO<sub>3</sub> based ferroelectric ceramics have become more significant in the electronic industry (Er et al., 2017).

Due to the numerous emission colors based on their 4f-4f or 5d-4f transitions, rare earth ions have been playing a significant role in modern lighting and display industries (Dutta et al., 2014). By doping BaTiO<sub>3</sub> with the appropriate metal ions at either the "A" or "B" sites, the ferroelectric, piezoelectric, and dielectric properties have been enhanced. In this regard, doping BaTiO<sub>3</sub> exposed the chance for its multifunctional properties by creating defects like oxygen vacancies (Adak et al., 2020). The effect of the sintering temperatures and processing conditions may result in the hexagonal polymorph being formed from normal perovskite-type barium titanate (You et al., 2020). One of the most crucial substitutions is using rare-earth dopants. (Taylor & Lin, 2012). Sm<sup>3+</sup> ions can penetrate into either the A-site or the B-site in

BaTiO<sub>3</sub> ceramics, which significantly influenced the dielectric characteristics and phase transition of these materials (Li et al., 2017).

The unit cell structure of BaTiO<sub>3</sub> ferroelectric materials has a positive charge center and a negative charge center that do not coincide, resulting in an electric dipole moment. This electric polarization causes spontaneous polarization within the crystals (Hamad, 2020).

The regulation of homogenous grain-growth in the material represents a crucial and beneficial task for technological applications because the majority of the useful features of BT-based ceramics are determined by the microstructural characteristics (i.e. grain-size) (Oliveira et al., 2019). In order to enhance the structural, dielectric, and electrical characteristics of BaTiO<sub>3</sub>, a number of synthetic techniques have been investigated, taking into account the creation of solid solutions and the addition of doping materials to the A- and/or B-site (Z. Li et al., 2005).

Dopants like La<sup>3+</sup>, Ce<sup>2+</sup>, Mn<sup>4+</sup> Ho<sup>3+</sup> and Dy<sup>3+</sup>, which have an intermediate range of ionic radius, can be added to BaTiO<sub>3</sub> to occupy Ba<sup>2+</sup> on A sites or Ti<sup>4+</sup> on B sites to form the solid solution, changing the material's microstructure and dielectric characteristics "function as either a donor or an acceptor" (Cai et al., 2011; Paunovic et al., 2016).

The BaTiO<sub>3</sub> defect chemistry for the incorporation of rare-earth ions depends primarily on the lattice site where the ion is substituted. The ions from the middle of the rare-earth series, such as Sm<sup>3+</sup>, exhibit amphoteric behavior, sometimes referred to as "magic dopants" and can occupy both cationic lattice sites in the BaTiO<sub>3</sub> structure (Properties, 2010; Alam et al., 2012).

Significant changes in the physical properties are facilitated by structural deformations and the creation of defects brought about by the inclusion of dopant elements into the BaTiO<sub>3</sub> perovskite structure. (Oliveira et al., 2019). BaTiO<sub>3</sub> ceramics are typically doped with Sm as an acceptor dopant integrated at the Ti<sup>4+</sup> site in order to lower the dielectric losses. Sm works to offset the effects of oxygen vacancies introduced by donors. (Paunovic et al., 2016).

With regard to the following rare-earth dopants in both Ba- and Ti-rich compositions, several researchers measured conductivity vs oxygen partial pressure over time: Er, Dy, Sm, Nd, Yb (Sur et al., 2001). According to literature data, the addition of Sm as a donor dopant in BaTiO<sub>3</sub> decreases the grain size and enhances the dielectric constant. Also, the addition of Sm causes lowering of the Curie temperature and a decrease of the dielectric losses (Paunovic et al., 2016).

The sol-gel procedure is a more chemical method (wet chemical method) for the creation of different nanostructures, particularly metal oxide nanoparticles (Bokov et al., 2021). Ceramics made of BaTiO<sub>3</sub> and Sm

were created using the traditional solid-state reaction technique.

Sm-doped BaTiO<sub>3</sub> ceramics' microstructure, dielectric, and ferroelectric characteristics have been studied. The outcome suggests that Sm<sup>3+</sup> ions enter the perovskite-type structure to replace Ba<sup>2+</sup> ions on the A sites, which results in a transition from a tetragonal to a cubic crystal structure. Samarium addition can prevent the formation of grains in ceramics made of BaTiO<sub>3</sub> and lower the Curie temperature (Taylor & Lin, 2012).

Powders of samarium-doped BaTiO<sub>3</sub> and pure barium titanate were prepared using a traditional solid-state technique. The effects of samarium addition on the development of the microstructure, grain growth inhibition, and structure modification were investigated. Doped samples' dielectric characteristics underwent significant modification. Doping caused a diffuse type of ferro-para phase transition, changed the sites of phase transitions, and decreased the dielectric permittivity values compared to pure barium titanate (Vijatovi et al., 2017).

The effect of the Sm-modifier concentration was studied in relation to the Pechini's method of producing BaTiO<sub>3</sub> ceramics. This synthesis procedure has been successful in producing nanosized crystallites that are between 15 and 20 nm in size. The X-ray diffraction technique was used to examine the structural properties, which revealed only one ferroelectric phase and no secondary phases. They also point to the amphoteric character of the Sm ion in the BaTiO<sub>3</sub> structure, which is shown by its occupancy of either the A- or B-sites (Oliveira et al., 2019).

In this paper, pure and Sm-doped BaTiO<sub>3</sub> ceramics were prepared by sol-gel technique and the Structural, Infra-red and Morphological effect of Sm<sup>3+</sup> doped BaTiO<sub>3</sub> effects were investigated, with (x = 0.0, 0.1, 0.2). We choose lower concentrations of "x" because higher concentrations could dominate the structure of the BaTiO<sub>3</sub>.

## MATERIALS AND METHODS

### Chemicals and reagents

The chemicals and reagents used are high-purity (99%–99.5%) analytic reagent (AR grade). The chemicals include, Barium nitrate [Ba (NO<sub>3</sub>)<sub>2</sub>] (Loba Chemie) Titanium dioxide (TiO<sub>2</sub>) (Loba Chemie) Samarium nitrate [Sm(NO<sub>3</sub>)<sub>2</sub>] (CDH) Citric acid (C<sub>6</sub>H<sub>8</sub>O<sub>7</sub>) (Loba Chemie) with distilled water as the solvent. All the chemicals and reagents were used as received without any further purification.

### Experimental details

The synthesis of Sm<sup>3+</sup> doped BaTiO<sub>3</sub> with chemical composition BaTi<sub>1-x</sub>Sm<sub>x</sub>O<sub>3</sub> (x = 0.0, 0.1, 0.2) have been successfully carried out using sol-gel technique. Appropriate amount of the chemicals was dissolved in 100ml of distilled water in stoichiometric ratios to form

an aqueous solution. The molar ratio of citric acid to cation was maintained at 1:2. The prepared solution was heated at a temperature of 80–100°C. The solution was stirred using constant and continuous magnetic stirring in order to evaporate the water; a light blue gel was obtained which was transferred to a hot plate and heated at a temperature of 280–300 °C. This gives a black precursor material which was grounded with mortar and pestle to obtain a fine BaTiSmO<sub>3</sub> precursor which was pre calcined in a digital controlled muffle furnace at 900°C for 5 h. The pre-calcinated powder was divided into three parts and labeled PQ1, PQ2, and PQ3. Furthermore, PQ1, PQ2 and PQ3 were further heated at 1100°C for 5 h respectively. The obtained product was crushed using mortar and pestle to obtain the fine BaTiSmO<sub>3</sub> ceramic powder followed by various characterizations.

#### Characterization techniques

X-ray diffraction pattern were carried out with a Bruker AXS D8 advanced XRD diffractometer to study the structural properties of the sample. Fourier transform infrared (FTIR) spectra obtained with Nicolet FTIR interferometer IR prestige-21 (model 8400S) was used to evaluate the functional groups. Field-emission scanning electron microscopy (FESEM/energy-dispersive X-ray (EDX) spectroscopy (FEI Nova NanoSEM 450 FE-SEM)/ at a voltage of 15 KV to determine the morphology and elemental analysis.

## RESULTS AND DISCUSSION

### XRD analysis

Fig. 1 shows the XRD pattern of BaTi<sub>1-x</sub>Sm<sub>x</sub>O<sub>3</sub>, ceramic powders calcined at 1100°C for 5 h. The diffraction peaks observed were indexed using JCPDS card number 79-2263 (Hai et al., 2014).

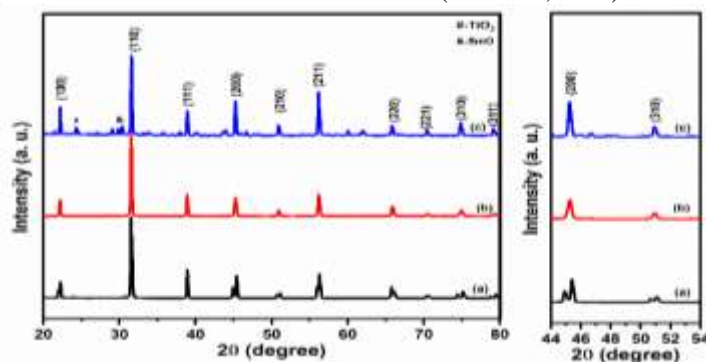


Figure 1: XRD patterns of BaTi<sub>1-x</sub>Sm<sub>x</sub>O<sub>3</sub> (x = 0.0, 0.1, 0.2).

From figure 1. (a) = x = 0.0, (b) = x = 0.1, and (c) = x = 0.2

The XRD results also suggest that doping ions like Sm<sup>3+</sup> can either occupy the lattice position of Ti<sup>4+</sup> at the B-site or Ba<sup>2+</sup> at the A site, respectively, in the perovskite structure. As Sm<sup>3+</sup> with an ionic radius of 0.95 Å is much smaller than Ba<sup>2+</sup> (1.35 Å) and is a little larger than Ti<sup>4+</sup> (0.605 Å). Therefore, an increase in “x” would result in an increase in interplanar crystal spacing and a decrease of X-ray diffraction peaks, including the (200) peak as reported by (Zhang et al., 2020). The (200) peak intensity declines with increasing Sm doping levels, suggesting that BST sample tetragonality declines with Sm concentration and the presence of cubic phase at high Sm content. This is because the replacement of Ti<sup>4+</sup> ions (0.605 Å) by the bigger Sm<sup>3+</sup> ions (0.958 Å) leading to the variation in cell parameter demonstrating the increase in lattice parameter with the increase of Sm content. As a result, the distortion in the structure of barium samarium doped samples diminishes with Sm content, changing the tetragonal structure of BST samples to a cubic structure as reported by (Hamad, 2020). However, for the compositions under study, it is possible to see the development of a minority phase (indicated by the symbols # and &) with typical reflections corresponding

to titanium oxide (TiO<sub>2</sub>) and samarium oxide (SmO) in the oxygen octahedral state, or the residual phase may be formed during the homogenization process with the citric acid in the formation of the final compound, indicating that the reaction has not yet been fully completed after the calc. According to the results reported in the literature, rare-earth ions with ionic radii (IR) between 0.87 Å and 0.94 Å could reveal some amphoteric character, which in fact strongly depends of the doping concentrations as reported by (Oliveira et al., 2019). Therefore, the obtained results for the XRD measurements suggest that ion replacing ionic radii of Ti<sup>4+</sup> (0.605 Å) by a larger one Sm<sup>3+</sup> (0.958 Å) at the octahedral B-site of the Sm<sup>3+</sup> ion behaves as an amphoteric element with substitutional character in both Ba- site and Ti-site of the perovskite structure of the BaTiO<sub>3</sub> system. The lattice constant (a) and volume of the unit cell (V<sub>cell</sub>) were calculated using the equations below.

$$a = d\sqrt{h^2 + k^2 + l^2} \quad (1)$$

$$V_{cell} = a^3 \quad (2)$$

where *d* is the interplanar spacing, *h*, *k* and *l* are the Miller indices. The lattice constant, the interplanar spacing and the volume of the unit cell are shown in the table 1 below. From the calculated table, it was found that the lattice

constant increases with increase in Ti-Sm concentrations, likewise, the volume of the unit cell increases with an increase in Ti-Sm concentrations. This may probably be caused by lattice distortion effect when the ionic

radius of the host ( $r_{Ti^{4+}} = 0.605\text{\AA}$ ) is replaced by ion with larger radius ( $r_{Sm^{3+}} = 0.958\text{\AA}$ ).

**Table 1: Interplanar spacing (d), lattice constant (a), and volume of the unit cell ( $v_{cell}$ ) of  $BaTi_{1-x}Sm_xO_3$  with  $x = 0.00, 0.10, \text{ and } 0.20$ . The Miller indices value (h k l) = (111).**

x	0.00	0.10	0.20
d (Å)	2.3051	2.3055	2.3063
a (Å)	3.9925	3.9932	3.9946
$v_{cell}$ (Å <sup>3</sup> )	63.6407	63.6742	63.7412

The tolerance factor of samarium doped  $BaTiO_3$  was calculated using the following equation (3) as shown in table 2.

$$t = (r_A + r_O) / \sqrt{2}(r_B + r_O) \quad (3)$$

where t is the tolerance factor.  $r_A$ ,  $r_B$  and  $r_O$  represent the ionic radii of the A site cation, the B-site cation and the oxygen anion respectively. The calculated tolerance value was 0.953 and 0.936 considering Sm-at B-site for  $BaTi_{1-x}Sm_xO_3$  indicating a cubic perovskite structure. Samarium is exclusively incorporated in the BT lattice on

the Ti site ( $0.605\text{\AA}$ ) and behaves as an acceptor according to the equation,  $Ti^{4+} \rightarrow Sm^{3+} + e^+$ .

### 3.2 FTIR Analysis

Fig. 2 shows the FTIR spectra of  $BaTi_{1-x}Sm_xO_3$  ( $x = 0.0, 0.1, 0.2$ ) in the wave number range  $500\text{--}4000\text{ cm}^{-1}$ . The formation of perovskite structure of the ceramic nanoparticles was supported by FTIR analysis. In order to determine the Sm-ion location (B-site), FTIR spectroscopy is utilized to know local deformations arising from the Sm doping.

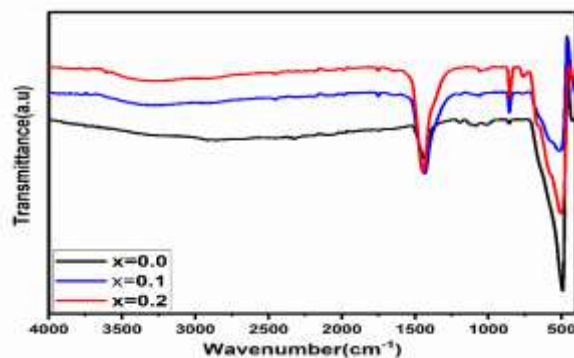


Figure 2: FTIR spectra of  $BaTi_{1-x}Sm_xO_3$  ( $x = 0.0, 0.1, 0.2$ ).

A strong absorption peak for pure BT powder is observed around  $493\text{ cm}^{-1}$ , signifying the stretching of normal vibration for Ti-O octahedron. Another absorption peaks for the same mode are observed at  $503$  and  $512\text{ cm}^{-1}$  for  $x = 0.1$  and  $0.2$  respectively. A shift toward higher frequency is observed due to the introduction of Sm at Ti site. The characteristic absorption band at  $1427, 1435$  and  $1443\text{ cm}^{-1}$  are assigned to symmetric stretching vibration for C-O, indicating that the citric acid react with BT during the preparation process which is not detected in XRD results as reported by (Hamad, 2020).

To examine the actual size and morphology of the particles, the samples were systematically analyzed by FESEM and EDX. Fig 3 (a) and (c) show the field

emission scanning electron microscopy micrographs of the sample  $BaTi_{1-x}Sm_xO_3$  ( $x = 0.0, \text{ and } 0.2$ ), prepared at  $1,100\text{ }^\circ\text{C}$  for 5 hours. micrographs confirm the presence of the polycrystalline microstructure with certain degree of porosity in good agreement with XRD results. Fig. 3 (b) and (d) show that the particles follow a normal distribution, with average particle sizes of  $73.5\text{ nm}$  and  $70.5\text{ nm}$  for  $x = 0.0$  and  $x = 0.2$  respectively, that is to say that the particle size decreases slightly with Sm concentrations. It is seen that the microstructures of all ceramics are dense and there is no obvious secondary phase structure observed, demonstrating that the sintering condition is appropriate doped  $BaTiO_3$  nanoparticles have been recorded.

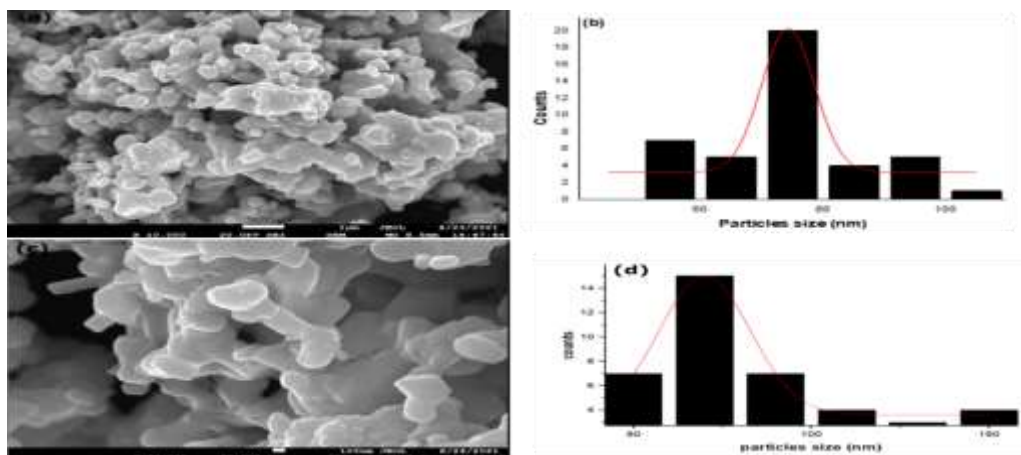


Figure 3: FESEM micrograph and particle distribution of  $\text{BaTi}_{1-x}\text{Sm}_x\text{O}_3$  ( $x = 0.00$ , and  $0.20$ ).

It is possible that the accumulation of  $\text{Sm}^{3+}$  ions close to the grain boundary, which inhibits grain growth during the sintering process, is what causes the reduction in grain size after doping the additives (Li et al., 2017). In comparison to samples of pure BT, the grain size is significantly smaller in those that contain Sm. Since it is discovered that the average grain size of pure BT is larger than the content of samarium doped BT. The substantial reduction in grain growth observed with Sm doping may be caused by Sm acceptance of electrons in the B-site, which reduces the likelihood of grain growth in the Sm

doped samples. This BT on Sm doping grain size reduction might improve the dielectric characteristics. The energy dispersive spectra of undoped as well as all the doped  $\text{BaTiO}_3$  nanoparticles have been recorded. A representative EDX spectrum of undoped and doped  $\text{BaTiO}_3$  is shown in Fig. 4 (a) and (b). It confirms the presence of Ba, Ti and O in our prepared sample. Spectra taken at a number of selected positions of the sample show the presence of the same constituents. The EDX spectrum of doped  $\text{BaTiO}_3$  confirmed the presence of all the dopant ions.

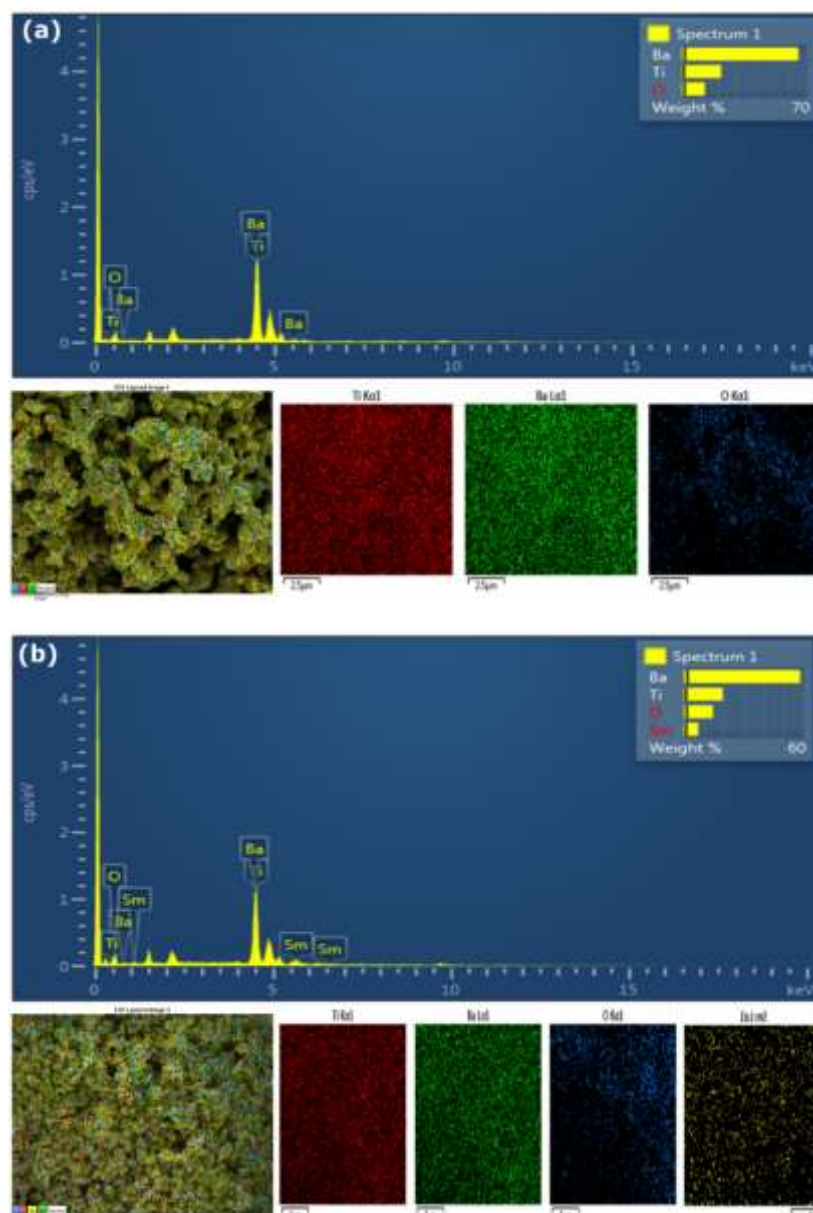


Figure 4: EDX spectra and mapping of BaTi<sub>1-x</sub>Sm<sub>x</sub>O<sub>3</sub> ( $x = 0.0$ , and  $0.2$ ).

The EDS spectra taken from different areas of the same sample, does not reveal any Sm rich regions thus indicating a uniform incorporation of dopants within the sample.

### CONCLUSION

Pure and Sm doped barium titanate ceramics were synthesized by the sol-gel method. Microstructural analysis showed nanometric size, which confirm the efficiency of the sol-gel auto combustion technique to obtain nano-powders based barium titanate samples. XRD results shows the replacement of Ti<sup>4+</sup> ions ( $0.605\text{\AA}$ ) by the bigger Sm<sup>3+</sup> ions ( $0.958\text{\AA}$ ) leading to the variation in cell parameter demonstrating the increase in lattice

parameter with the increase of Sm content. The calculated tolerance value was 0.952 considering Sm-at B-site for BaTi<sub>1-x</sub>Sm<sub>x</sub>O<sub>3</sub> indicating a cubic perovskite structure, a strong absorption peak for pure BT powder is observed around  $493\text{cm}^{-1}$ , signifying the stretching of normal vibration for Ti-O octahedron. Another absorption peaks for the same mode are observed at  $503$  and  $512\text{cm}^{-1}$  for  $x = 0.1$  and  $0.2$  respectively. The X-ray diffraction results, FESEM show that the particles follow a normal distribution, with average particle sizes of  $73.5\text{nm}$  and  $70.5\text{nm}$  for  $x = 0.0$  and  $x = 0.2$  respectively, that is to say that the particle size decreases slightly with Sm concentrations, EDX spectra confirms the presence

of Ba, Ti, O and dopant in our prepared sample of the same constituents.

#### ACKNOWLEDGEMENT

The authors are grateful to the Materials Research Centre, Malaviya National Institute of technology, Jaipur, India, for FESEM/EDX spectroscopy, XRD, FTIR characterizations.

#### CONFLICT OF INTEREST

The author declares no conflict of interest.

#### REFERENCES

Adak, M. K., Mondal, D., Mondal, S., Kar, S., Mahato, S. J., Mahato, U., Gorai, U. R., Ghorai, U. K., & Dhak, D. (2020). Materials Science & Engineering B Ferroelectric and photocatalytic behavior of Mn- and Ce-doped BaTiO<sub>3</sub> nanoceramics prepared by chemical route. *Materials Science & Engineering B*, 262(September), 114800. <https://doi.org/10.1016/j.mseb.2020.114800>

Alam, M. A., Zuga, L., & Pecht, M. G. (2012). *CERAMICS Economics of rare earth elements in ceramic capacitors*.

Bokov, D., Jalil, A. T., Chupradit, S., Suksatan, W., Ansari, M. J., Shewael, I. H., Valiev, G. H., & Kianfar, E. (2021). *Nanomaterial by Sol-Gel Method : Synthesis and Application. 2021*.

Cai, W., Fu, C. L., Gao, J. C., & Zhao, C. X. (2011). *Dielectric properties and microstructure of Mg doped barium titanate ceramics*. 110(3), 181–185. <https://doi.org/10.1179/1743676110Y.0000000019>

Dutta, D. P., Ballal, A., Nuwad, J., & Tyagi, A. K. (2014). Optical properties of sonochemically synthesized rare earth ions doped BaTiO<sub>3</sub> nanophosphors: Probable candidate for white light emission. *Journal of Luminescence*, 148, 230–237. <https://doi.org/10.1016/j.jlumin.2013.11.071>

Er, B., Ismail, F. A., Aina, R., Osman, M., Idris, M. S., Taking, S., Azhar, Z., & Jamal, Z. (2017). *Dielectric and microstructural properties of. 01051*, 5–9. <https://doi.org/10.1051/epjconf/201716201051>

Hai, C., Inukai, K., Takahashi, Y., Izu, N., Akamatsu, T., Itoh, T., & Shin, W. (2014). Surfactant-assisted synthesis of mono-dispersed cubic BaTiO<sub>3</sub> nanoparticles. *Materials Research Bulletin*, 57, 103–109. <https://doi.org/10.1016/j.materresbull.2014.05.036>

Hamad, M. A. (2020). Characterization of excessive Sm<sup>3+</sup> containing barium titanate prepared by tartrate

precursor method. *Journal of Materials Research and Technology*, 9(6), 15214–15221. <https://doi.org/10.1016/j.jmrt.2020.10.015>

Li, Y., Dun, W., Yan, S., Zuo, G., & Qu, Y. (2017). Effect of samarium and lanthanum co-dopant on the microstructure and dielectric properties of -. *Journal of Materials Science: Materials in Electronics*, 0(0), 0. <https://doi.org/10.1007/s10854-017-6966-7>

Li, Z., Zhang, H., Zou, X., & Bergman, B. (2005). *Synthesis of Sm-doped BaTiO<sub>3</sub> ceramics and characterization of a secondary phase*. 116, 34–39. <https://doi.org/10.1016/j.mseb.2004.09.017>

Oliveira, M. A., M, J. C., Hernandez, A. C., Guo, R., Bhalla, S., Guerra, J. D. S., M, J. C., & Hernandez, A. C. (2019). Structural and microstructural analyses on Sm-modified BaTiO<sub>3</sub> obtained from the Pechini's method. *Ferroelectrics*, 533(1), 99–107. <https://doi.org/10.1080/00150193.2018.1470819>

Paunovic, V., Mitic, V. V., & Kocic, L. (2016). *Dielectric characteristics of donor-acceptor modified BaTiO<sub>3</sub> ceramics*. <https://doi.org/10.1016/j.ceramint.2016.04.087>

Properties, C. E. (2010). *Influence of Rare-Earth Dopants on Barium Titanate Ceramics Microstructure and Corresponding Electrical Properties*. 137(25042), 132–137. <https://doi.org/10.1111/j.1551-2916.2009.03309.x>

Smith, M. B., Page, K., Siegrist, T., Redmond, P. L., Walter, E. C., Seshadri, R., Brus, L. E., Steigerwald, M. L., Barbara, S., Laboratories, B., Mountain, A. V., & Hill, M. (2008). *Crystal Structure and the Paraelectric-to-Ferroelectric Phase Transition of Nanoscale BaTiO<sub>3</sub>*. 14, 6955–6963.

Sur, Y. T., Itomi, A. H., Crymgeour, I. S., & Andall, C. A. R. (2001). *Site Occupancy of Rare-Earth Cations in BaTiO<sub>3</sub>*. 40(1), 255–258.

Taylor, P., & Lin, Z. (2012). *Integrated Ferroelectrics : An Effect of Samarium on the Microstructure , Dielectric and Ferroelectric Properties of Barium Titanate Ceramics Effect of Samarium on the Microstructure , Dielectric and Ferroelectric Properties of Barium*. April 2013, 37–41. <https://doi.org/10.1080/10584587.2012.741466>

Vijatovi, M. M., Grigalaitis, R., Ilic, N., & Bobi, J. D. (2017). *Interdependence between structure and electrical characteristics in Sm-doped barium titanate*. 724. <https://doi.org/10.1016/j.jallcom.2017.07.099>

You, A., Be, M. A. Y., & In, I. (2020). *Dielectric and*

*structural analysis of hexagonal and tetragonal phase BaTiO<sub>3</sub> Dielectric and Structural Analysis of Hexagonal and. 020038(*January), 1–8.

Zhang, B., Lou, X., Zheng, K., Xie, X., Shi, P., Guo, M.,

Zhu, X., Gao, Y., Liu, Q., & Kang, R. (2020). Enhanced electrocaloric effect in the Sm and Hf co-doped BaTiO<sub>3</sub> ceramics. *Ceramics International*, July. <https://doi.org/10.1016/j.ceramint.2020.08.226>